

17 **ABSTRACT**

18 A persistent challenge in enhancing gene therapy is the transient availability of the target gene
19 product. This is particularly true in tissue engineering applications. The transient exposure of
20 cells to the product could be insufficient to promote tissue regeneration. Here we report the
21 development of a new material engineered to have a high affinity for a therapeutic gene product.
22 We focus on insulin-like growth factor-I (IGF-I) for its highly anabolic effects on many tissues
23 such as spinal cord, heart, brain and cartilage. One of the ways that tissues store IGF-I is through
24 a group of insulin like growth factor binding proteins (IGFBPs), such as IGFBP-5. We grafted
25 the IGF-I binding peptide sequence from IGFBP-5 onto alginate in order to retain the
26 endogenous IGF-I produced by transfected chondrocytes. This novel material bound IGF-I and
27 released the growth factor for at least 30 days in culture. We found that this binding enhanced the
28 biosynthesis of transfected cells up to 19-fold. These data demonstrate the coordinated
29 engineering of cell behavior and material chemistry to greatly enhance extracellular matrix
30 synthesis and tissue assembly, and can serve as a template for the enhanced performance of other
31 therapeutic proteins.

32

33

34

35

36

37

38

39

40

41

42

43

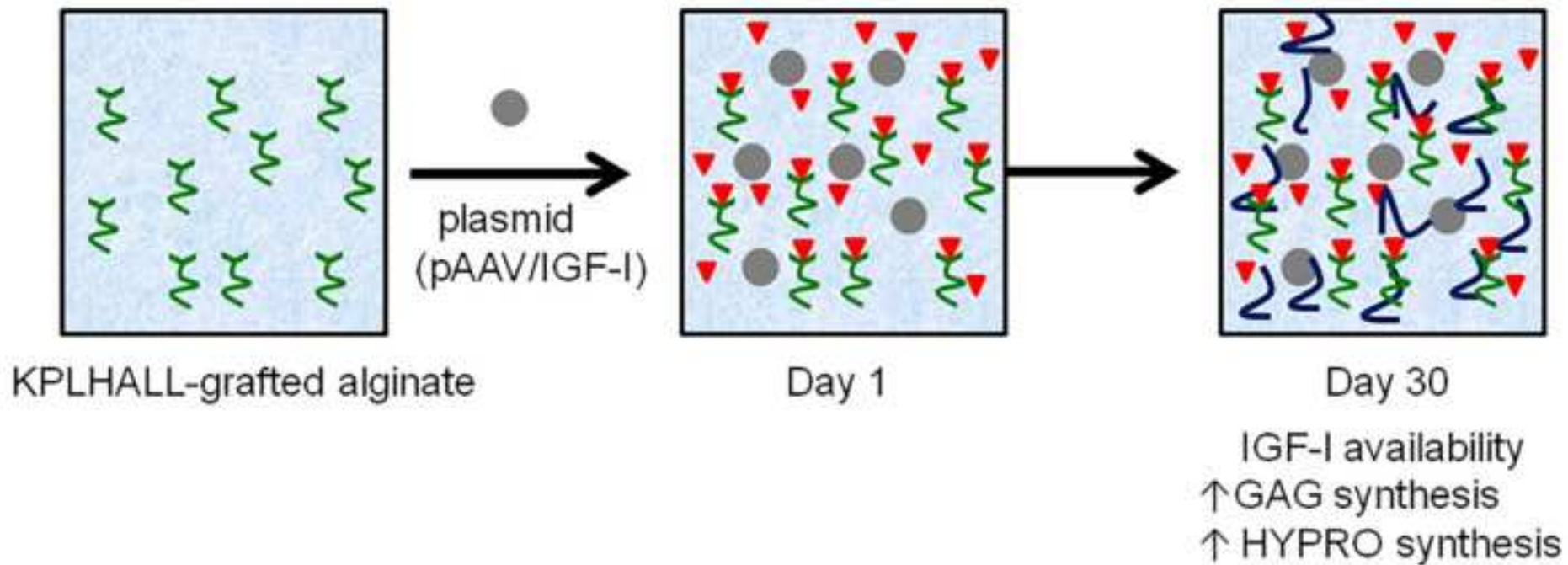
44

● Transfected Chondrocyte with Plasmid (pAAV/IGF-I)

⌘ KPLHALL Peptide from the IGFBP-5

▼ IGF-I

⌘ ECM Production



45 **1. INTRODUCTION**

46 A number of recent studies have focused on delivering therapeutic proteins using gene
47 therapy to enhance the repair of skeletal muscle, brain, spinal cord, and cartilage[1–3]. Many of
48 these studies have focused on a variety of membrane repair proteins, transcription factors, and
49 growth factors to increase cellular synthesis and control paracrine cascades[1,4,5]. However, one
50 of the main limiting factors in the efficacy of gene therapy is the transient availability of the gene
51 product, regardless of the vector used. For example the use of gene therapy in cartilage repair has
52 targeted increased growth factor production; however, the desired gene product is typically
53 upregulated for up to two weeks[6,7]. Further, the highest concentrations of growth factors are in
54 the first days after transfection, and have the potential to produce supra-therapeutic, or toxic
55 levels of the growth factor[8].

56 One of the proteins commonly targeted for cartilage repair in gene therapy is insulin-like
57 growth factor–I (IGF-I)[7–10]. Various viral and nonviral vectors have been used to
58 transduce/transfect chondrocytes to upregulate IGF-I synthesis prior to therapeutic cell
59 delivery[7,11–13]. Although IGF-I expression can remain elevated for a month or more[14], this
60 expression decreases with time, and is often low by 2 weeks[7,15]. This is an extremely short
61 time compared to the 6-12 months typically needed for effective cartilage repair[16], and may
62 not induce optimal repair *in vivo*. As such, there is a great need for approaches to extend the
63 availability of IGF-I for cartilage therapy.

64 In tissues such as cartilage, IGF-I is retained in the tissue by a family of binding proteins
65 called insulin-like growth factor binding proteins (IGFBPs). These binding proteins are highly
66 specific to IGF-I, with binding affinities of 1-10 nM[17]. IGFBPs also bind to cartilage enhanced
67 cellular matrix (ECM), acting as both a sink and source for the growth factor as needed[18]. It

68 has been shown that IGFBP-5 has a specific localized small domain that is largely responsible
69 for its high affinity binding to IGF-I[17].

70 Cell-based gene therapy for articular cartilage repair requires a means of delivering cells to the
71 site in need of repair[19]. There has been increased attention to the development of biomaterials
72 that prolong release and expression of gene products. Some of those biomaterials are chitosan,
73 poly-L-lactic acid (PLLA), poly(3-hydroxybutyrate-co-3-hydroxyhexanoate) (PHBHHx),
74 polyethylenimine (PEI), and polyethyleneglycol (PEG). Chondrocytes have been cultured in
75 chitosan-fabricate and a plasmid DNA scaffold to study cell proliferation, adherence, and
76 transforming growth factor- β 1 (TGF- β 1) expression[20] and chitosan-pEGFP nanoparticles have
77 been used to transfer exogenous genes into primary chondrocytes for the treatment of joint
78 diseases[21]. Trimethylated chitosan (TMO) was synthesized from oligometric chitosan to
79 deliver luciferase plasmid DNA to epithelial cells[22]. PLLA has been used with mesenchymal
80 stem cells (MSCs) transfected with adenoviral SOX-9 to differentiate monolayer MSCs into
81 chondrocyte-like cells[23]. PHBHHx scaffolds have been seeded with chondrocytes which
82 employed tetracycline (Tet-on) to induce Sox9 expression[24]. Modified polyethylenimine (PEI)
83 exhibited lower toxicity and higher gene expression of plasmid DNA in COS-7 cells and
84 HepG2cells[25]. Polyethylene glycol-grafted polyethylenimine (PEG-PEI) has been used as a
85 vector to deliver gene products to adipose stem cells to differentiate them to cartilage or
86 osteoblast cells[26]. Hydrogels, including alginate, have also been shown to serve this
87 purpose[27]. There are numerous examples of short peptide sequences being grafted to materials
88 to enhance cell adhesion[17,28,29]. Similarly, materials have been modified to contain heparin-
89 like carbohydrate components which have been shown to enhance binding of growth factors such
90 as FGF-2[30]. All of the previous materials have been used to promote gene delivery and to

91 prolong the release and expression of the gene product, but none of these materials have
92 interacted in any specific way with the proteins that are targeted for production by the cells. The
93 goal of this study was to develop a material that could bind to the targeted gene product and
94 assess whether that binding will enhance matrix production. To our knowledge, peptide-based
95 modification of materials to localize growth factors has not been reported.

96 Here we demonstrate the development of a new material with high affinity for IGF-I by
97 grafting a binding peptide sequence from IGFBP-5 onto alginate. This new material greatly
98 extends the availability of the growth factor during chondrocyte culture and enhances cartilage
99 matrix biosynthesis up to 19-fold.

100

101 **2. MATERIALS AND METHODS**

102 *2.1 Chemistry*

103 UP LVG alginate (from NovaMatrix®) was modified with carbodiimide chemistry[28].
104 100 mg alginate (1% w/v alginate solution) was dissolved in 0.1 M of 1-(*N*-morpholino)
105 ethanesulfonic acid (MES) buffer (Sigma-Aldrich) at pH 6.5. The reaction scheme is shown in
106 Figure 1 where amide linkages were obtained by adding 2.5 mM of 1-ethyl-
107 (dimethylaminopropyl) carbodiimide (EDC) (Sigma-Aldrich) and 1.2 mM of sulfo-*N*-
108 hydroxysuccinimide (NHS) to raise the efficiency of amide bond formation (Pierce
109 Chemical)[28]. 1 mg of GGG-K(ivDde)PLALL peptide sequence (INNOVAGEN) was added
110 after 5 minutes; the solution was left to react for 20 hrs. The reaction was quenched with 0.026
111 mM of hydroxyamine hydrochloride (Sigma-Aldrich) at 20 hrs. Alginate solution was purified
112 by dialysis (3500 MWCO) (Fisher Scientific) with different salt concentrations varying 115 mM
113 to 0 mM. Samples were stored at -80 °F for 24 hours and then they were lyophilized for 24

114 hours. The additional 3 glycines at the N- terminus of this synthetic peptide sequence were added
115 in order to provide a linker layer that would more fully expose the active peptides in the
116 sequence once the peptide was bound to a surface. The lysine on this sequence was protected
117 from unwanted chemical reactions by an ivDde protecting group; this was removed using 5%
118 hydrazine, anhydrous (Sigma) in dimethylformamide (DMF). Following the deprotection step,
119 the modified alginate solution GGG-KPLALL (KPLHALL) was purified by dialysis (3500
120 MWCO) (Fisher Scientific) with DI H₂O for 24 hours. Samples were stored at -80 °F for 24
121 hours and then they were lyophilized for 24 hours.

122 *2.2 Nuclear Magnetic Resonance Studies*

123 The freeze-dried KPLHALL alginate and unmodified alginate were dissolved in D₂O at
124 0.0012% w/v. There were three groups: alginate, a mixture of alginate with free KPLHALL
125 peptide, and KPLHALL-grafted alginate. ¹H nuclear magnetic resonance (¹H NMR) spectra were
126 recorded on 600MHz Varian Inova NMR. ¹H NMR was normalized to residual solvent D₂O. The
127 final molar concentration of peptide KPLHALL grafted in alginate was obtained by integrating
128 the area under the curve with MNova NMR Software, 100 μM of binding sites of KPLHALL
129 (0.3% of degree of graft on alginate backbone). Also, diffusion ordered spectroscopy (DOSY)
130 was performed to demonstrate stable attachment of the peptide sequence to the alginate.

131 *2.3 Surface Plasmon Resonance Studies*

132 Surface Plasmon Resonance (SPR) measurements were performed with an SPR
133 Refractometer Instrument (Reichert, Inc., Depew, NY). A range of KPLHALL concentrations
134 from 0 to 100 μM was achieved by mixing the 100 μM KPLHALL with unmodified alginate in
135 varying ratios. Modified and unmodified alginate were bound to 50 nm thick gold chips (Fischer
136 Scientific, Pittsburg, PA) using carbodiimide chemistry. Samples were run at 25° C in buffer for

137 10 minutes per sample, using a constant flow rate of 25 μl /min over the surface of the SPR chip.
 138 Concentrations of IGF-I ranged from 5 to 3000 nM. PBST (PBS plus 0.05% v/v Tween 20) was
 139 used as both the sample and flow buffer. After each binding experiment, the surface was
 140 regenerated with 40 mM HCl. The sensorgram profiles were analyzed using SigmaPlot where
 141 response to equilibrium was calculated with an three parameter exponential rise to maximum
 142 model and then a Langumir binding model was used to determine the binding constant (K_D) [31].

143 2.4 Analysis

144 The microrefractive index unit at equilibrium was measured for each concentration of IGF-I as it
 145 flowed through the chip (Equation 1).

$$R(t) = R_{eq} \left(1 - e^{\left(\frac{t-t_0}{\tau} \right)} \right)$$

146 Where, R_{eq} is the refractive index unit at equilibrium, t is time, t_0 is the time after baseline, and
 147 τ is the exponential time constant.

148 K_D was calculated by fitting the data to Langmuir's Affinity Kinetics Model [31] (Equation 2)

$$R_{eq} = \frac{[IGF - I] * R_{max}}{[IGF - I] + K}$$

149
 150 R_{eq} is the response at equilibrium for each curve; [IGF-I] is the concentration of IGF-I; R_{max} is
 151 the maximum equilibrium response and K_D is the binding affinity constant. The dissociation rate
 152 constant (k_{off}) was calculated by fitting the dissociation phase[31] (Equation 3)

$$R_T = (R_{eq} - R_{off}) \left(1 - e^{\left(\frac{t-t_1}{k_{off}} \right)} \right)$$

153 Where, R_T is the total response where it is assumed that the total complex concentration of IGF-I
 154 and KPLHALL $[IGF-I * KPLHALL]_{TOTAL}$ is proportional to the total response (RT). R_{eq} is the
 155 response at equilibrium for each curve and R_{off} is the equilibrium response at the end of the

156 dissociation phase. The experiment was measured at different times, t (time where dissociation
157 finished) and t_1 (time where dissociation started).

158 Furthermore, the association rate constant (k_{on}) of each IGF-I concentration was calculated as
159 (Equation 4)

$$K = \frac{k_{off}}{k_{on}}$$

160

161 2.5 Cell Culture and Matrix Synthesis:

162 Chondrocytes were isolated as previously described[7,32]. Articular cartilage was
163 harvested from stifle (knee) condyles of 1-3 day old bovids (*Bos taurus*). Articular cartilage was
164 washed with PBS and 1% antibiotics and antimycotic. Chondrocytes were then isolated by
165 adding 0.3% type 2 collagenase (catalogue number LS004177, Worthington Biochemical,
166 Lakewood, NJ) overnight. Isolated chondrocytes were washed and suspended in DMEM
167 containing 100 U/mL penicillin, 100 μ g/mL streptomycin, and 10% fetal bovine serum (FBS)
168 and placed in T-75 flasks plates at 60% confluency at 37°C in 5% CO₂. After 48 hours, cells
169 were transfected using two different complexes, made 30 minutes before transfection, at a ratio
170 of 3:1[7,10,33]: FuGENE[®]6 (Roche Applied Science, Indianapolis, IN) + pAAV/IGF-I or
171 FuGENE[®]6+pAAV/ MCS (Empty). After 16 hours, the transfection was stopped by replacing
172 the culture medium with 5 mL of fresh media without FBS, and 100 U/mL penicillin, 100 μ g/mL
173 streptomycin. Afterwards, cells were trypsinized and mixed with 2% (w/v) modified or
174 unmodified alginate. These culture, encapsulation, and transfection methods were selected based
175 on previous work [9] demonstrating the successful formation of tissue in vivo using these
176 protocols.

177 A range of KPLHALL concentrations from 0 to 100 μM was achieved by mixing the 100
 178 μM KPLHALL with unmodified alginate in varying ratios. Cells were encapsulated in beads
 179 formed by extrusion through a 22-gauge needle into a 102 mM CaCl_2 solution. Beads were
 180 incubated with DMEM without FBS for 30 days; beads were collected every six days.

181 2.6 Biochemical Analysis

182 Beads collected every six days for 30 days were used to measure DNA,
 183 glycosaminoglycan (GAG) and hydroxyproline (HYPRO) content. DNA content was measured
 184 via Hoechst dye assay[34]. GAG content was measured using the DMMB dye-binding assay[35],
 185 and HYPRO content was measured using DMAB dye assay[36]. Syntheses of GAG [35] and
 186 HYPRO [36] were used as the primary measure of chondrocyte metabolic activity. The kinetics
 187 of GAG and HYPRO accumulation were fitted to an established model of matrix synthesis to
 188 calculate steady-state GAG and HYPRO content [37] (Equation 5).

$$[ECM](t) = [ECM]_{SS} \left(1 - e^{-\frac{t}{\tau}}\right)$$

189 Where, [ECM] is the matrix synthesized by the transfected or control of chondrocytes in
 190 the different concentrations of KPLHALL. $[ECM]_{SS}$ is steady state matrix production produced
 191 by the chondrocytes at different concentrations of KPLHALL. Each steady state value was
 192 normalized to alginate (0 μM) steady state value for GAG and HYPRO. These normalized
 193 steady-state values of GAG and HYPRO synthesis were used to determine the effect of
 194 KPLHALL content on chondrocyte matrix synthesis using a generalized variable slope
 195 concentration–response model (Equation 6) [37].

$$\frac{[ECM]_{SS}}{[ECM]_{0\mu\text{M}}_{SS}} = [ECM]_{min} + \frac{[ECM]_{max} - [ECM]_{min}}{1 + \left(\frac{[KPLHALL]}{EC_{50}}\right)^{-Hillslope}}$$

196 Where, $[ECM]_{SS}$ is the steady state matrix production, $[ECM]_{0\mu\text{M}}_{SS}$ is the steady state matrix
 197 production, $[ECM]_{max}$ is the maximum stimulation, $[ECM]_{min}$ is the minimum stimulation,

198 [KPLHALL] is the concentration of KPLHALL- modified alginate, and EC_{50} is the dose required
199 to produce 50% response.

200 Beads from day 30 were collected for immunohistochemistry analysis. Samples were
201 treated with citrate antigen retrieval buffer for 10 minutes at 90°C. Slides were then washed with
202 TBS/TWEEN20 and PBS. Samples were placed in humidity chambers for 30 minutes with 3%
203 hydrogen peroxide. Blocking solution (goat serum) was added and incubated for 1 hour at room
204 temperature. Afterwards the primary antibody Rb pAb for IGF-I (ab40657) was applied and left
205 overnight at 4°C. Negative controls were obtained by omitting the primary antibody to a section
206 on each slide (See supplementary figure S1). Next Rabbit IgG for secondary antibody was
207 applied for 30 minutes at room temperature, followed by ABC reagent (Vectastain PK-4000,
208 Vector Labs). Slides were developed with DAB peroxidase (Vector Labs) for approximately 3
209 minutes.

210 *2.7 Statistical Analysis*

211 GAG and HYPRO data are expressed as mean \pm SD. The effect of culture time and
212 transfection were analyzed by 2-way ANOVA using Tukey's t-test for post hoc analysis
213 performed in SigmaPlot 11 (SYSTAT, Chicago, IL), with significance determined with $p < 0.05$.

214 The temporal patterns in GAG and HYPRO data were then fit to equation 5 using SigmaPlot 11,
215 which calculated best fit values of $[ECM]_{SS}$ and τ , with the uncertainties in these fits expressed as
216 standard error.

217 Each steady state values and standard errors were normalized to alginate (0 μ M) steady
218 state value for GAG and HYPRO. The normalized values were fitted to Equation 6 using
219 software SigmaPlot 11, which enabled the calculation of best fit values for EC_{50} , $[ECM]_{max}$, and
220 $[ECM]_{min}$ values and their uncertainty, expressed as standard error. Statistical differences

221 between EC_{50} , $[ECM]_{max}$, and $[ECM]_{min}$ were determined by an unpaired t test using GradPad
222 Prism (GraphPad, Inc., La Jolla, CA).

223

224 3. RESULTS

225 *3.1 Generation and Characterization of Hydrogels with Affinity for IGF-I*

226 The peptide sequence KPLHALL from the hydrophobic binding pocket of IGFBP-5 was
227 chosen as a candidate for enhancing IGF-I binding based on analysis of the crystal structure of
228 IGFBP-5 /IGF-I complex. These data showed that 6 of the 7 amino acids in this peptide sequence
229 were within 4Å of IGF-I when the complex is formed, enabling a high level of affinity [38].

230 The high affinity sequence was synthesized and grafted to alginate via previously
231 established carbodiimide/sulfo-NHS chemistry[39](Fig 1A). The modification of alginate was
232 confirmed by 1H NMR analysis, using the leucine peaks at ~0.7 ppm to both demonstrate
233 successful grafting and measure the amount of conjugated peptide (Fig 1B). Additionally the
234 stability of the peptide graft was demonstrated by diffusion ordered NMR (DOSY), which
235 showed the persistence of leucine peaks in the grafted material (See supplementary figure S2).

236 Analysis of IGF-I binding to modified and control alginate via surface plasmon resonance
237 (SPR) demonstrated significant enhancement of binding by the modified material (Fig1C). The
238 dissociation constant (K_D) decreased from 513 nM to 50 nM due to modification with
239 KPLHALL (Fig1C). This level of affinity for IGF-I was lower than that for full length of
240 IGFBP-5 ($K_D=3.7$ nM), but similar to a truncated form of IGFBP-5 containing only the binding
241 pocket ($K_D=37$ nM)[17].

242 *3.2 Enhancement of IGF-I Binding and Matrix Production*

243 The enhanced binding demonstrated by KPLHALL-modified alginate motivated the
244 hypothesis that this material would retain IGF-I produced by encapsulated chondrocytes. To test
245 this hypothesis, articular chondrocytes were transfected with an adeno-associated virus-based
246 plasmid vector (pAAV/IGF-I), carrying human IGF-I cDNA (transfected chondrocytes) or with
247 empty vector (control chondrocytes) and encapsulated as previously described[33,39] in
248 modified and unmodified alginate and cultured for 30 days.

249 We have previously shown that IGF-I transfection is highly efficient, but also transient,
250 with enhanced IGF-I expression subsiding within 6 days[7,33]. Consistent with this data,
251 immunohistochemistry staining of unmodified alginate (i.e. 0 μ M binding peptide) cultures
252 showed minimal presence of IGF-I at 30 days (Fig.2). In contrast, control chondrocytes cultured
253 in alginate modified with KPLHALL showed enhanced retention of IGF-I at 30 days, with IGF-I
254 retention proportional to the concentration of the grafted binding peptide. This enhancement was
255 greater in chondrocytes transfected with pAAV/IGF-I, where the highest concentrations of
256 binding peptide (i.e. 33 μ M and 100 μ M) resulted in robust staining for IGF-I at 30 days (Fig.2).

257 Both empty vector control and pAAV/IGF-I transfected chondrocytes showed
258 accumulation of the principal cartilage matrix components with time. Transfection with
259 p/AAV/IGF-I enhanced accumulation of glycosaminoglycan (GAG) ($p < 0.001$ by 2-way
260 ANOVA) (Fig3A) and collagen, as indicated by hydroxyproline (HYPRO) ($p < 0.001$) when
261 compared to empty vector controls (Fig.3B). These typically reached steady state after two
262 weeks in culture. The average of the time constants (τ) varied from 5.4 ± 3.6 hr to 10.0 ± 8.0 hr
263 for GAG; tau values varied from 3.0 ± 3.7 hr to 27.9 ± 7.2 hr for HYPRO. The presence of
264 peptide binding enhanced matrix synthesis in empty vector and pAAV/IGF-I transfected cultures
265 (* $p < 0.001$ by 2-way ANOVA) for both GAG and HYPRO. In IGF-I transfection had a dramatic

266 effect on HYPRO production both in the presence and absence of the binding peptide (*p<0.01
267 by 2-way ANOVA).

268 To understand the effect of IGF-I retention via binding peptide sites, the steady-state
269 matrix contents were calculated using an established kinetic model [37]. For each culture
270 condition, steady state matrix contents were normalized to the unmodified alginate (0 μ M),
271 which revealed that matrix synthesis was clearly dose-dependent ($R^2>0.93$ for all fits) on binding
272 peptide density (Fig.4A). For the control cells, enhancement of GAG and HYPRO synthesis
273 were 1.6 and 3-fold, respectively. This effect was more dramatic in transfected cells, with GAG
274 and HYPRO synthesis upregulated 6.9 (*p<0.0001 by unpaired t test) and 19.4-fold (%p<0.02 by
275 unpaired t test), respectively. For all cultures, EC_{50} for enhancement of synthesis ranged from 17
276 to 41 μ M KPLHALL.

277 **4. DISCUSSION**

278 These data illustrate that the biomimetic modification of alginate with a binding peptide
279 from IGFBP-5 enables high affinity binding of IGF-I. The data further demonstrate that this
280 modification extend the presence of the growth factor in cell-seeded constructs to at least one
281 month, and that this extended presence of IGF-I in turn substantially enhances cartilage matrix
282 synthesis.

283 Producing materials that specifically bind IGF-I present specific technical challenges.
284 Proteins that are known to bind IGF-I have complex 3D configurations that stabilize the
285 formation of the binding protein-IGF-I complex[38]. IGFBP-5, which has 252 residues, and
286 mini-IGFBP-5, which has 52 residues, have binding affinities of 3.7 nM and 37 nM respectively.
287 Grafting such proteins to a material to enhance IGF-I binding would be technically challenging
288 and expensive, due to the cost of producing the protein recombinantly. Additionally, stability of

289 the grafted material would be of great concern. Grafting shorter peptides would solve this
290 problem; however it is not clear whether shorter peptides would produce high affinity binding.
291 Here we showed that grafting a seven peptide sequence from the binding pocket of IGFBP-5 to
292 alginate produced a material with high affinity ($K_D = 50$ nM). This peptide sequence is short
293 enough that folding is likely absent or minimally important. However, it is important to note that
294 grafting to alginate via the ϵ amino group in the lysine residue of the peptide rather than the
295 glycine leader sequence eliminated the beneficial effect on matrix synthesis (data not shown).
296 This data suggests that some amount of leader sequence is necessary for proper binding of IGF-I
297 to the modified alginate. Additionally, the affinity may be aided by the fact that alginate is a
298 polyanion and IGF-I is positively charged ($pI = 8.5$) [40], and charge based interaction may play
299 a role in aiding binding. Nevertheless the significant enhancement of IGF-I binding by the
300 addition of a short peptide may provide a template for targeted modification of biomaterials for
301 growth factor binding.

302 Other studies have explored alternative approaches for expanding the time of IGF-I
303 action through controlled delivery. For example, the interaction of IGF-I with the cartilage ECM
304 has been altered by generating a recombinant fusion protein of IGF-I with a heparin binding
305 domain[41]. This modified IGF-I bound to heparin sulfate and chondroitin sulfate with high
306 affinities (21 nM and 172 nM) and extended the retention time of the growth factor in
307 cartilage[41]. Other approaches for delivery include gene-activated matrix (GAM) [42]
308 materials, in which a material is loaded with a plasmid that is released slowly to the cells.
309 Similarly IGF-I peptide was released from degradable microparticles to achieve delivery over ~2
310 weeks[43]. The approach described in the current paper compliments these previously described

311 approaches and provides additional flexibility for tuning both cellular and matrix responses over
312 many weeks. Additionally, we can use our modified alginate with other methods of gene therapy.

313 Similarly this modified material may be helpful in enhancing other methods of gene
314 therapy. Many studies on cartilage gene therapy have focused on extending the time of
315 production and availability of IGF-I. Adeno-associated virus (AAV), a non-pathogenic human
316 parvovirus, is capable of transfecting non-dividing cells for extended periods of time and can
317 transduce normal and osteoarthritic articular cartilage *in vitro*[44]. Adenoviral vectors (Ade.IGF-
318 I) have been used to transduce cells where production of IGF-I ranges from 21 days up to 150
319 days[45,46]. Also, chondrocytes transduced with recombinant adeno-associated virus
320 (rAAV)[47] have produced IGF-I for over 20 days. While our approach described here focused
321 on plasmid transfection, such an approach can also be used with any of the above vectors.
322 Tuning both IGF-I production and binding could enable even more extended availability of the
323 growth factor.

324 Both IGF-I as a target growth factor[48,49] and alginate as a delivery vehicle[50,51] have
325 been used *in vivo* to enhance the repair of cartilage. The modified alginate presented here shows
326 great promise to further improve chondrocyte matrix production and cartilage repair *in vivo*[50].
327 We noted a robust staining for type II collagen, particularly at higher concentrations of
328 KPLHALL constructs (See supplementary figure S3). Furthermore, the DNA analysis showed
329 similar amounts of DNA throughout all the groups throughout the duration of the experiments.
330 This data, in combination with the matrix synthesis data suggests that a relatively uniform
331 number of cells was maintained during culture (See supplementary figure S4). This new
332 biomaterial can be incorporated into other studies that have used alginate as a scaffold or have
333 used other vectors[48,52]. Overall, these data suggest that combining gene therapy with targeted

334 modification of scaffold material provides a platform where cellular production and extracellular
335 binding of IGF-I act synergistically to enhance cellular biosynthesis. IGF-I regulates many other
336 tissues including spinal cord[53], heart[54] and brain[55,56]. As such, these studies suggest the
337 possibility of using such modified biomaterial not only with chondrocytes, but with other cell
338 types. Furthermore, this approach can be extracted for use with other growth factors, such as
339 TGF- β and BMP-2, that also have known protein binding sites in extracellular matrix[57,58].

340 **5. CONCLUSION**

341 Modifying alginate with the peptide KPLHALL from the binding pocket of IGFBP-5
342 enhanced binding affinity more than 10-fold, extended IGF-I availability over 30 days and
343 increased GAG and HYPRO synthesis 7 and 20 fold respectively. The approach of controlling
344 growth factor binding, by the grafting of small peptides for biomaterials represents an important
345 new approach to drug delivery and tissue engineering.

346

347 **Figure Captions**

348 **Figure 1**

349 **1A Reaction Scheme:** EDC and Sulfo-NHS activate the alginate forming a carboxylate carbon
350 intermediate. The carboxylate carbon intermediate is attacked by the primary amine nitrogen
351 forming the amide bond to the alginate backbone.

352 **1B NMR Spectra:** First spectra shows the alginate sample with broad peaks for a
353 polysaccharide, from 4.8 to 3.2, and distinct peak for the anomeric proton[59]. Second spectrum,
354 mixture of the alginate and peptide, shows both different peaks for alginate and high leucine
355 amino acids peaks. The third spectrum shows the modified alginate with KPLHALL where the
356 chemical shift in the leucine peaks and the height of the peaks differs from the mixture.

357 **1C SPR Spectra and Langmuir's Affinity Kinetics Model:** Representative examples of curve
358 fits for the affinity kinetic analysis of control (alginate) and modified alginate (KPLHALL
359 alginate). Concentrations of IGF-I for alginate varied from 3000 nM to 0 nM. Concentrations of
360 IGF-I for KPLHALL alginate varied from 1000 nM to 0 nM.

361 Langmuir's Affinity Kinetics Model for alginate is the top one (blue) and KPLHALL alginate is
362 on the bottom (red). K_D shifted 10 times, where K_D is 50 nM sin KPLHALL alginate (K_D of 50
363 nM) when compared to alginate (K_D of 513 nM). KPLHALL alginate had a k_{on} ranging from 1 to
364 $4(10^8/M \cdot sec)$ and a k_{off} from 5/s to 19/s (R^2 : 0.40 to 0.90). The parameters for alginate k_{on} and
365 k_{off} ranged from 1.6 to $1.8(10^8/Ms)$ and k_{off} 10/s to 29/s (R^2 : 0.74 to 0.9).

366 **Figure 2**

367 **IGF-I Binding**

368 Immunohistochemistry of constructs for IGF-I at Day 30. Scale bar = 100 μm . Alginate does not
369 show differences in immunolocalization staining at day 30. Immunolocalization staining for IGF-
370 I changes as the concentration of binding sites (KPLHALL) increases in the constructs. The
371 constructs with 0 μM of binding sites barely show retention of f IGF-I; and constructs with 1 and
372 3 μM of binding sites show some retention of IGF-I. The highest immunolocalization of IGF-I is
373 at 100 μM .

374 **Figure 3**

375 **3A GAG matrix accumulation kinetic profiles:** The production of GAG increases in both
376 transfected and control groups. Control chondrocytes have smaller changes in kinetic profiles
377 between the differences in KPLHALL concentrations. pAAV/IGF-I transfected chondrocytes
378 have a greater effect ($*p < 0.001$ by 2-way ANOVA) between the differences in KPLHALL
379 concentrations.

380 **3B HYPRO matrix accumulation kinetic profiles:** The production of HYPRO increases in
381 both pAAV/IGF-I transfected chondrocytes and control chondrocytes. The effect in
382 chondrocytes that are transfected with pAAV/IGF-I is greater than the effect on those transfected
383 with pAAV/ MCS (Empty) ($p < 0.001$ by 2-way ANOVA). This effect is greater in concentrations
384 of 10, 33 and 100 μM binding sites ($p < 0.001$ by 2-way ANOVA). When alginate is compared
385 with the highest concentration of binding sites (100 μM) there is an increase from 0.08 $\mu\text{g}/\text{mg}$ at
386 0 μM to 1.4 $\mu\text{g}/\text{mg}$ at 100 μM ($p < 0.001$ by 2-way ANOVA) in pAAV/IGF-I transfected
387 chondrocytes.

388 **Figure 4**

389 **4A GAG and HYPRO Dose Response:** GAG at the steady state concentration of each
390 concentration is plotted against the different concentrations of binding sites of KPLHALL
391 covalently attached to alginate. Transfected chondrocytes with pAAV/IGF-I produce 600%
392 GAG, than the control chondrocytes transfected with pAAV/ MCS (Empty) ($*p < 0.0001$ by
393 unpaired t test). pAAV/IGF-I transfected chondrocytes required 16.9 μM of binding sites in the
394 alginate to produce an increase in GAG of 6.9 (Table 2). Control chondrocytes required almost
395 twice the amount of KPLHALL modified alginate only to produce 60% (Table 2). $*p < 0.001$
396 when compared to min. $+p < 0.001$ when compared to max empty.

397 **4B Dose Response:** The production of HYPRO increases both in pAAV/IGF-I transfected
398 chondrocytes and control chondrocytes. The effect in chondrocytes that are transfected with
399 pAAV/IGF-I is greater than the effect in cells transfected with pAAV/ MCS (Empty).
400 pAAV/IGF-I increased HYPRO accumulation by 20 fold at the maximum effective
401 concentration of IGF-I binding sites ($p < 0.02$ by unpaired t test). The parameters are summarized

402 on table 2 where all R^2 are higher than 0.93 (Table 2). % $p < 0.02$ when compared to min. $^{\wedge}p < 0.02$
403 when compared to max empty.

404 **Supplemental 1**

405 Negative Control for IGF-I IHC in 100 μ M KPLHALL Alginate with pAAV/IGF-I transfected
406 chondrocytes. Scale bar = 100 μ m

407 **Supplemental 2**

408 Diffusion NMR was performed to see the stability of conjugation in the alginate; the NMR signal
409 of the leucines is present even as the gradient increases. In contrast to the mixture sample, the
410 leucine signals disappear as the gradient increases.

411 **Supplemental 3**

412 Immunohistochemistry of constructs for type II collagen at Day 30. Scale bar = 100 μ m

413 Robust staining for type II collagen, particularly at higher concentrations of KPLHALL
414 constructs.

415 **Supplemental 4**

416 Amount of DNA via Hoechst DNA assay throughout the duration of the experiment.

417

418

419

420

421

422

423

424

425 **ACKNOWLEDGMENTS**

426 This research is supported by Alfred P. Sloan Foundation, Coleman Foundation, Award
427 NIH/NIAMS F31AR061982, NIH Grant R01 AR047702, and the Department of Veterans
428 Affairs. We would like to thank Dr. Keresztes for his help with the NMR, Dr. Parker for all her
429 help with the SPR and Ms. Michele Karr for all her help.

430

431 **REFERENCES**

- 432 [1] N. Weisleder, N. Takizawa, P. Lin, X. Wang, C. Cao, Y. Zhang, T. Tan, C. Ferrante, H. Zhu, P.-J.
433 Chen, R. Yan, M. Sterling, X. Zhao, M. Hwang, M. Takeshima, C. Cai, H. Cheng, H. Takeshima,
434 R.-P. Xiao, J. Ma, Recombinant MG53 Protein Modulates Therapeutic Cell Membrane Repair in
435 Treatment of Muscular Dystrophy, *Sci. Transl. Med.* 4 (2012) 139ra85–139.
436 doi:10.1126/scitranslmed.3003921.
- 437 [2] A.H. Nagahara, D. a Merrill, G. Coppola, S. Tsukada, B.E. Schroeder, G.M. Shaked, L. Wang, A.
438 Blesch, A. Kim, J.M. Conner, E. Rockenstein, M. V Chao, E.H. Koo, D. Geschwind, E. Masliah,
439 A. a Chiba, M.H. Tuszynski, Neuroprotective effects of brain-derived neurotrophic factor in
440 rodent and primate models of Alzheimer’s disease., *Nat. Med.* 15 (2009) 331–337.
441 doi:10.1038/nm.1912.
- 442 [3] K. Bartus, N.D. James, A. Didangelos, K.D. Bosch, J. Verhaagen, R.J. Yáñez-Muñoz, J.H. Rogers,
443 B.L. Schneider, E.M. Muir, E.J. Bradbury, Large-Scale Chondroitin Sulfate Proteoglycan
444 Digestion with Chondroitinase Gene Therapy Leads to Reduced Pathology and Modulates
445 Macrophage Phenotype following Spinal Cord Contusion Injury., *J. Neurosci.* 34 (2014) 4822–36.
446 doi:10.1523/JNEUROSCI.4369-13.2014.
- 447 [4] W. Kafienah, F. Al-Fayez, A.P. Hollander, M.D. Barker, Inhibition of cartilage degradation: A
448 combined tissue engineering and gene therapy approach, *Arthritis Rheum.* 48 (2003) 709–718.
449 doi:10.1002/art.10842.
- 450 [5] C.H. Evans, J.N. Gouze, E. Gouze, P.D. Robbins, S.C. Ghivizzani, Osteoarthritis gene therapy.,
451 *Gene Ther.* 11 (2004) 379–89. doi:10.1038/sj.gt.3302196.
- 452 [6] a J. Nixon, R. a Saxer, B.D. Brower-Toland, Exogenous insulin-like growth factor-I stimulates an
453 autoinductive IGF-I autocrine/paracrine response in chondrocytes., *J. Orthop. Res.* 19 (2001) 26–
454 32. doi:10.1016/S0736-0266(00)00013-9.
- 455 [7] S. Shi, S. Mercer, S.B. Trippel, Effect of transfection strategy on growth factor overexpression by
456 articular chondrocytes., *J. Orthop. Res.* 28 (2010) 103–9.
- 457 [8] P. Yu, X. Wang, Y.X. Fu, Enhanced local delivery with reduced systemic toxicity: delivery,
458 delivery, and delivery., *Gene Ther.* 13 (2006) 1131–1132. doi:10.1038/sj.gt.3302760.

- 459 [9] H. Madry, D. Zurakowski, S.B. Trippel, Overexpression of human insulin-like growth factor-I
460 promotes new tissue formation in an ex vivo model of articular chondrocyte transplantation., *Gene*
461 *Ther.* 8 (2001) 1443–9.
- 462 [10] H. Madry, G. Kaul, M. Cucchiari, U. Stein, D. Zurakowski, K. Remberger, M.D. Menger, D.
463 Kohn, S.B. Trippel, Enhanced repair of articular cartilage defects in vivo by transplanted
464 chondrocytes overexpressing insulin-like growth factor I (IGF-I)., *Gene Ther.* 12 (2005) 1171–9.
- 465 [11] R.A. Saxer, S.J. Bent, B.D. Brower-Toland, Z. Mi, P.D. Robbins, C.H. Evans, a J. Nixon, Gene
466 mediated insulin-like growth factor-I delivery to the synovium., *J. Orthop. Res.* 19 (2001) 759–67.
- 467 [12] H. Madry, M. Cucchiari, Advances and challenges in gene-based approaches for osteoarthritis.,
468 *J. Gene Med.* 15 (2013) 343–55. doi:10.1002/jgm.2741.
- 469 [13] I. Hellgren, V. Drvota, R. Pieper, S. Enoksson, P. Blomberg, K.B. Islam, C. Sylvén, Highly
470 efficient cell-mediated gene transfer using non-viral vectors and FuGene6: in vitro and in vivo
471 studies., *Cell. Mol. Life Sci.* 57 (2000) 1326–33. <http://www.ncbi.nlm.nih.gov/pubmed/11028922>.
- 472 [14] L.R. Goodrich, C. Hidaka, P.D. Robbins, C.H. Evans, A.J. Nixon, Genetic modification of
473 chondrocytes with insulin-like growth factor-1 enhances cartilage healing in an equine model., *J.*
474 *Bone Joint Surg. Br.* 89 (2007) 672–685. doi:10.1302/0301-620X.89B5.18343.
- 475 [15] B.D. Brower-Toland, R. a Saxer, L.R. Goodrich, Z. Mi, P.D. Robbins, C.H. Evans, a J. Nixon,
476 Direct adenovirus-mediated insulin-like growth factor I gene transfer enhances transplant
477 chondrocyte function., *Hum. Gene Ther.* 12 (2001) 117–29.
- 478 [16] Brigham, Standard of Care : Autologous Chondrocyte Implantation (ACI), 34 (2007) 1–8.
- 479 [17] W. Kalus, M. Zweckstetter, C. Renner, Y. Sanchez, J. Georgescu, M. Grol, D. Demuth, R.
480 Schumacher, C. Dony, K. Lang, T. a Holak, Structure of the IGF-binding domain of the insulin-
481 like growth factor-binding protein-5 (IGFBP-5): implications for IGF and IGF-I receptor
482 interactions., *EMBO J.* 17 (1998) 6558–72. doi:10.1093/emboj/17.22.6558.
- 483 [18] J.I. Jones, A. Gockerman, W.H. Busby, C. Camacho-Hubner, D.R. Clemmons, Extracellular
484 matrix contains insulin-like growth factor binding protein-5: potentiation of the effects of IGF-I.,
485 *J. Cell Biol.* 121 (1993) 679–87.
- 486 [19] P. Ducheyne, R.L. Mauck, D.H. Smith, Biomaterials in the repair of sports injuries., *Nat. Mater.*
487 11 (2012) 652–4. doi:10.1038/nmat3392.
- 488 [20] T. Guo, J. Zhao, J. Chang, Z. Ding, H. Hong, J. Chen, J. Zhang, Porous chitosan-gelatin scaffold
489 containing plasmid DNA encoding transforming growth factor- β 1 for chondrocytes proliferation,
490 *Biomaterials.* 27 (2006) 1095–1103. doi:10.1016/j.biomaterials.2005.08.015.
- 491 [21] X. Zhao, S.B. Yu, F.L. Wu, Z. Bin Mao, C.L. Yu, Transfection of primary chondrocytes using
492 chitosan-pEGFP nanoparticles, *J. Control. Release.* 112 (2006) 223–228.
493 doi:10.1016/j.jconrel.2006.01.016.

- 494 [22] M. Thanou, B.I. Florea, M. Geldof, H.E. Junginger, G. Borchard, Quaternized chitosan oligomers
495 as novel gene delivery vectors in epithelial cell lines, *Biomaterials*. 23 (2002) 153–159.
- 496 [23] S.M. Richardson, J.M. Curran, R. Chen, A. Vaughan-Thomas, J. a. Hunt, A.J. Freemont, J.A.
497 Hoyland, The differentiation of bone marrow mesenchymal stem cells into chondrocyte-like cells
498 on poly-L-lactic acid (PLLA) scaffolds, *Biomaterials*. 27 (2006) 4069–4078.
499 doi:10.1016/j.biomaterials.2006.03.017.
- 500 [24] Y. Yao, Y. He, Q. Guan, Q. Wu, *Biomaterials* A tetracycline expression system in combination
501 with Sox9 for cartilage tissue engineering, *Biomaterials*. 35 (2014) 1898–1906.
502 doi:10.1016/j.biomaterials.2013.11.043.
- 503 [25] C. Liu, P. Zhang, X. Zhai, F. Tian, W. Li, J. Yang, Y. Liu, H. Wang, W. Wang, W. Liu,
504 *Biomaterials* Nano-carrier for gene delivery and bioimaging based on carbon dots with PEI-
505 passivation enhanced fluorescence, *Biomaterials*. 33 (2012) 3604–3613.
506 doi:10.1016/j.biomaterials.2012.01.052.
- 507 [26] X.A. Chen, L.J. Zhang, Z.J. He, W.W. Wang, B. Xu, Q. Zhong, X.T. Shuai, L.Q. Yang, Y. Bin
508 Deng, Plasmid-encapsulated polyethylene glycol-grafted polyethylenimine nanoparticles for gene
509 delivery into rat mesenchymal stem cells., *Int. J. Nanomedicine*. 6 (2011) 843–853.
510 doi:10.2147/IJN.S17155.
- 511 [27] H. Madry, M. Cucchiari, U. Stein, K. Remberger, M.D. Menger, D. Kohn, S.B. Trippel,
512 Sustained transgene expression in cartilage defects in vivo after transplantation of articular
513 chondrocytes modified by lipid-mediated gene transfer in a gel suspension delivery system., *J.*
514 *Gene Med.* 5 (2003) 502–9.
- 515 [28] J. a Rowley, G. Madlambayan, D.J. Mooney, Alginate hydrogels as synthetic extracellular matrix
516 materials., *Biomaterials*. 20 (1999) 45–53.
- 517 [29] D.L. Hern, J. a. Hubbell, Incorporation of adhesion peptides into nonadhesive hydrogels useful for
518 tissue resurfacing, *J. Biomed. Mater. Res.* 39 (1998) 266–276. doi:10.1002/(SICI)1097-
519 4636(199802)39:2<266::AID-JBM14>3.0.CO;2-B.
- 520 [30] J. a Marcum, R.D. Rosenberg, Anticoagulant active heparin-like molecules from vascular
521 tissue., *Biochemistry*. 23 (1984) 1730–1737. doi:10.1016/0014-4827(86)90525-2.
- 522 [31] N.; Packer, N.; Karlsson, *Surface Plasmon Resonance Methods and Protocols, Methods in*
523 *Molecular Biology*, 2010. doi:10.1007/978-1-60761-670-2.
- 524 [32] J.J. Ballyns, T.M. Wright, L.J. Bonassar, Effect of media mixing on ECM assembly and
525 mechanical properties of anatomically-shaped tissue engineered meniscus., *Biomaterials*. 31
526 (2010) 6756–63. doi:10.1016/j.biomaterials.2010.05.039.
- 527 [33] I.N. Aguilar, S. Trippel, L.J. Bonassar, Comparison of Efficacy of Endogenous and Exogenous
528 IGF-I in Stimulating Matrix Production in Neonatal and Mature Chondrocytes, 14853 (2015) 1–
529 22. doi:10.1177/1947603515578691.

- 530 [34] G.A. Kim YJ, Sah R, Doongoe-Yuan H, Fluorometric Assay of DNA in Cartilage Explants Using
531 Hoechst 33258 Cartilage Explant Sample Preparation, *Anal. Biochemistry*. 174 (1988) 168–176.
- 532 [35] B.O. Enobakhare, D.L. Bader, D.A. Lee, Quantification of Sulfated Glycosaminoglycans in
533 Chondrocyte / Alginate Cultures , by Use of 1,9 Dimethylmethylene Blue, *Anal. Biochemistry*. 243
534 (1996) 191–194.
- 535 [36] R.E. Neuman, M.A. Logan, The determination of hydroxyproline, *J. Biol. Chem.* (1949) 229–306.
536 doi:10.1016/0009-8981(65)90038-0.
- 537 [37] W. Sauermaun, T.J. Feuerstein, Some Mathematical Models for Concentration-Response
538 Relationships, *Biometrical J.* 40 (1998) 865–881.
- 539 [38] W. Zesławski, H.G. Beisel, M. Kamionka, W. Kalus, R. a Engh, R. Huber, K. Lang, T. a Holak,
540 The interaction of insulin-like growth factor-I with the N-terminal domain of IGFBP-5., *EMBO J.*
541 20 (2001) 3638–44. doi:10.1093/emboj/20.14.3638.
- 542 [39] N.G. Genes, J. a Rowley, D.J. Mooney, L.J. Bonassar, Effect of substrate mechanics on
543 chondrocyte adhesion to modified alginate surfaces., *Arch. Biochem. Biophys.* 422 (2004) 161–7.
544 doi:10.1016/j.abb.2003.11.023.
- 545 [40] L.M. Mullen, S.M. Best, R. a Brooks, S. Ghose, J.H. Gwynne, J. Wardale, N. Rushton, R.E.
546 Cameron, Binding and release characteristics of insulin-like growth factor-1 from a collagen-
547 glycosaminoglycan scaffold., *Tissue Eng. Part C. Methods*. 16 (2010) 1439–48.
548 doi:10.1089/ten.TEC.2009.0806.
- 549 [41] R. Miller, A.J. Grodzinsky, K. Cummings, A. Plaas, A. Cole, R.T. Lee, P. Patwari, M.D.D. Sc,
550 Intra-articular Injection of HB-IGF-1 Sustains Delivery of IGF-1 to Cartilage through Binding to
551 Chondroitin Sulfate, 62 (2011) 3686–3694. doi:10.1002/art.27709.Intra-articular.
- 552 [42] J. Bonadio, Tissue engineering via local gene delivery, *J. Mol. Med.* 78 (2000) 303–311.
553 doi:10.1007/s001090000118.
- 554 [43] J. Elisseeff, W. McIntosh, K. Fu, B.T. Blunk, R. Langer, Controlled-release of IGF-I and TGF-
555 beta1 in a photopolymerizing hydrogel for cartilage tissue engineering., *J. Orthop. Res.* 19 (2001)
556 1098–1104. doi:10.1016/S0736-0266(01)00054-7.
- 557 [44] H. Madry, M. Cucchiariini, E.F. Terwilliger, S.B. Trippel, Recombinant adeno-associated virus
558 vectors efficiently and persistently transduce chondrocytes in normal and osteoarthritic human
559 articular cartilage., *Hum. Gene Ther.* 14 (2003) 393–402. doi:10.1089/104303403321208998.
- 560 [45] A.F. Steinert, G.D. Palmer, C. Pilapil, U. Nöth, C.H. Evans, S.C. Ghivizzani, Enhanced in vitro
561 chondrogenesis of primary mesenchymal stem cells by combined gene transfer., *Tissue Eng. Part*
562 *A.* 15 (2009) 1127–1139. doi:10.1089/ten.tea.2007.0252.
- 563 [46] H. Madry, M. Cucchiariini, E.F. Terwilliger, S.B. Trippel, Recombinant adeno-associated virus
564 vectors efficiently and persistently transduce chondrocytes in normal and osteoarthritic human
565 articular cartilage., *Hum. Gene Ther.* 14 (2003) 393–402. doi:10.1089/104303403321208998.

- 566 [47] A. Weimer, H. Madry, J.K. Venkatesan, G. Schmitt, J. Frisch, A. Wezel, J. Jung, D. Kohn, E.F.
567 Terwilliger, S.B. Trippel, M. Cucchiarini, Benefits of recombinant adeno-associated virus
568 (rAAV)-mediated insulinlike growth factor I (IGF-I) overexpression for the long-term
569 reconstruction of human osteoarthritic cartilage by modulation of the IGF-I axis., *Mol. Med.* 18
570 (2012) 346–58. doi:10.2119/molmed.2011.00371.
- 571 [48] A.J. Nixon, L.A. Fortier, J. Williams, H. Mohammed, Enhanced Repair of Extensive Articular
572 Defects by Insulin-like Growth Factor-I-laden Fibrin Composites, (1999).
- 573 [49] L.J. Bonassar, a J. Grodzinsky, E.H. Frank, S.G. Davila, N.R. Bhaktav, S.B. Trippel, The effect of
574 dynamic compression on the response of articular cartilage to insulin-like growth factor-I., *J.*
575 *Orthop. Res.* 19 (2001) 11–7. doi:10.1016/S0736-0266(00)00004-8.
- 576 [50] G. Kaul, M. Cucchiarini, D. Arntzen, D. Zurakowski, M.D. Menger, D. Kohn, S.B. Trippel, H.
577 Madry, Local stimulation of articular cartilage repair by transplantation of encapsulated
578 chondrocytes overexpressing human fibroblast growth factor 2 (FGF-2) in vivo., *J. Gene Med.* 8
579 (2006) 100–11. doi:10.1002/jgm.819.
- 580 [51] K.Y. Lee, M.C. Peters, K.W. Anderson, D.J. Mooney, Controlled growth factor release from
581 synthetic extracellular matrices., *Nature.* 408 (2000) 998–1000. doi:10.1038/35050141.
- 582 [52] H. Madry, M. Cucchiarini, G. Kaul, D. Kohn, E.F. Terwilliger, S.B. Trippel, T. SB, Menisci Are
583 Efficiently Transduced by Recombinant Adeno-Associated Virus Vectors In Vitro and In Vivo,
584 *Am. J. Sports Med.* 32 (2004) 1860–1865.
- 585 [53] G.L. Hinks, R.J. Franklin, Distinctive patterns of PDGF-A, FGF-2, IGF-I, and TGF-beta1 gene
586 expression during remyelination of experimentally-induced spinal cord demyelination., *Mol. Cell.*
587 *Neurosci.* 14 (1999) 153–168. doi:10.1006/mcne.1999.0771.
- 588 [54] O.S. Opgaard, P.H. Wang, IGF-I is a matter of heart, *Growth Horm. IGF Res.* 15 (2005) 89–94.
589 doi:10.1016/j.ghir.2005.02.002.
- 590 [55] E. Carro, J.L. Trejo, T. Gomez-Isla, D. LeRoith, I. Torres-Aleman, Serum insulin-like growth
591 factor I regulates brain amyloid-beta levels., *Nat. Med.* 8 (2002) 1390–1397. doi:10.1038/nm793.
- 592 [56] S. Doré, S. Kar, R. Quirion, Rediscovering an old friend, IGF-I: potential use in the treatment of
593 neurodegenerative diseases., *Trends Neurosci.* 20 (1997) 326–331. doi:S0166223696010363 [pii].
- 594 [57] S. Schultz-Cherry, S. Ribeiro, L. Gentry, J.E. Murphy-ullrich, Thrombospondin Binds and
595 Activates the Small and Large Forms of Latent Transforming Growth Factor-b in a Chemically
596 Defined System, *J. Biol. Chem.* 269 (1994) 26775–26782.
- 597 [58] a. Sweatt, D.C. Sane, S.M. Hutson, R. Wallin, Matrix Gla protein (MGP) and bone morphogenetic
598 protein-2 in aortic calcified lesions of aging rats, *J. Thromb. Haemost.* 1 (2003) 178–185.
599 doi:10.1046/j.1538-7836.2003.00023.x.
- 600 [59] D.J. Mooney, Presentation of BMP - 2 Mimicking Peptides in 3D Hydrogels Directs Cell Fate
601 Commitment in Osteoblasts and Mesenchymal Stem Cells, (2013).

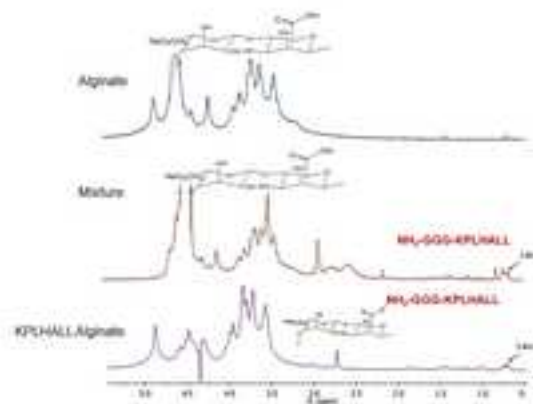
Figure 1

[Click here to download high resolution image](#)

A) Reaction Scheme



B) ¹H NMR Spectra



C) SPR Analysis

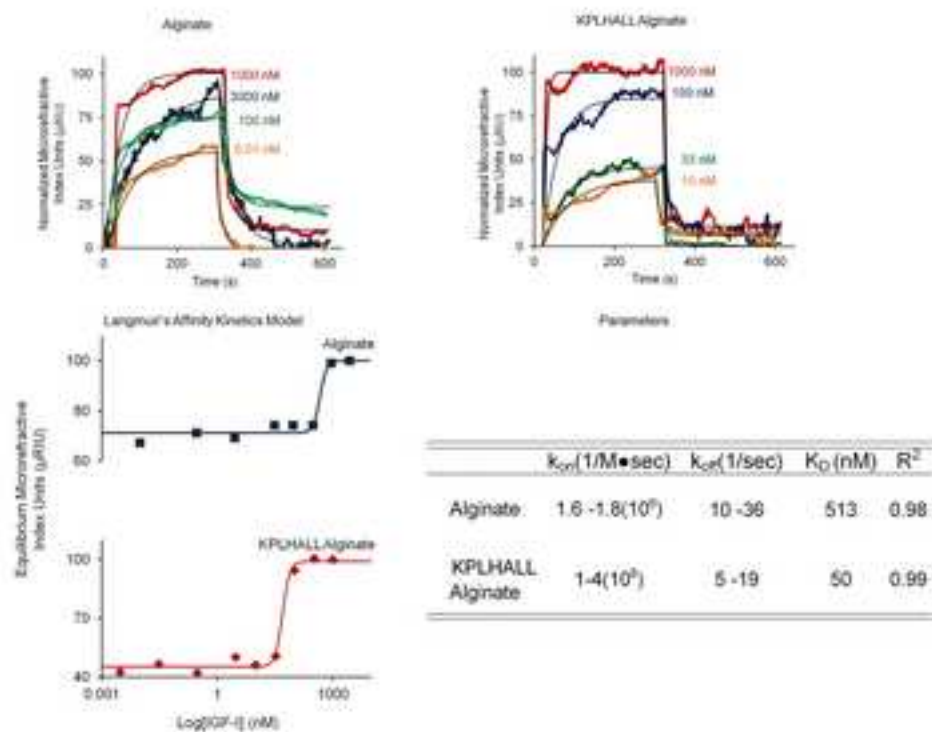
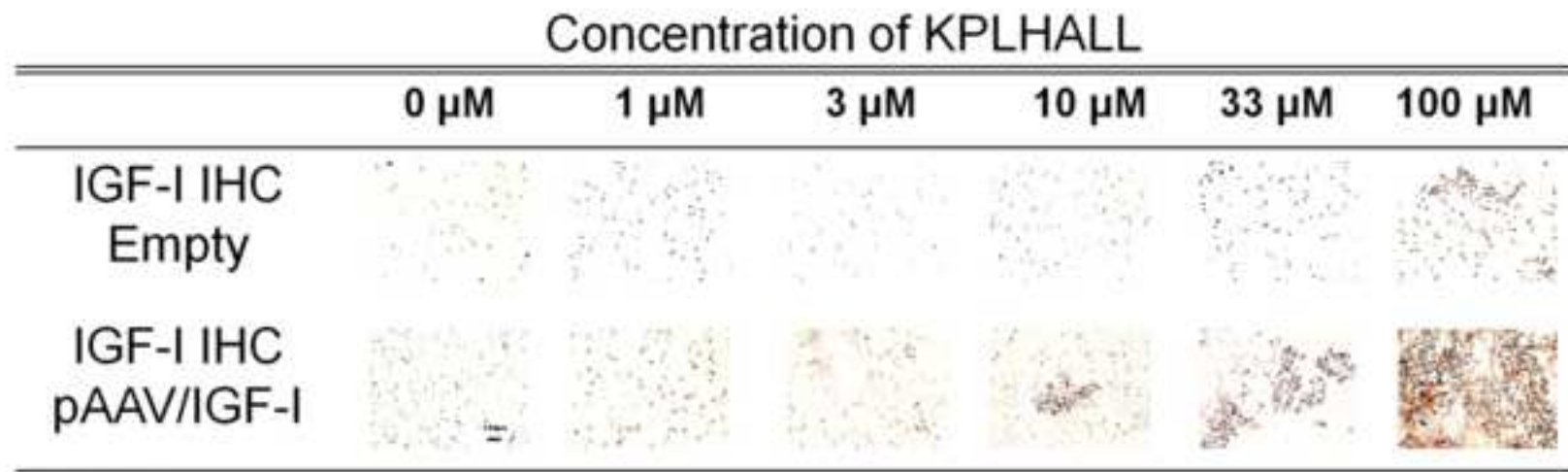
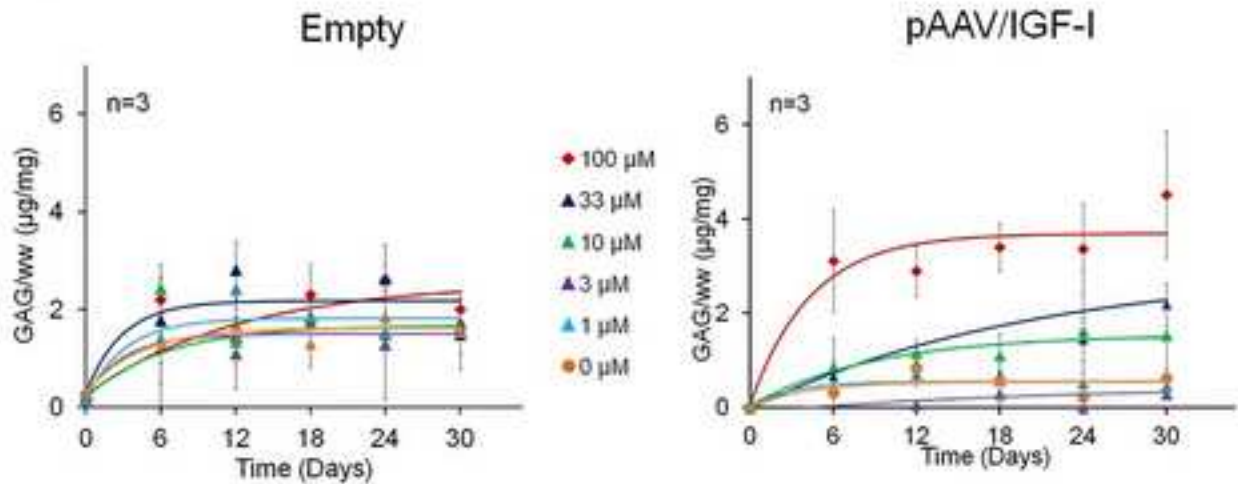


Figure 2
[Click here to download high resolution image](#)

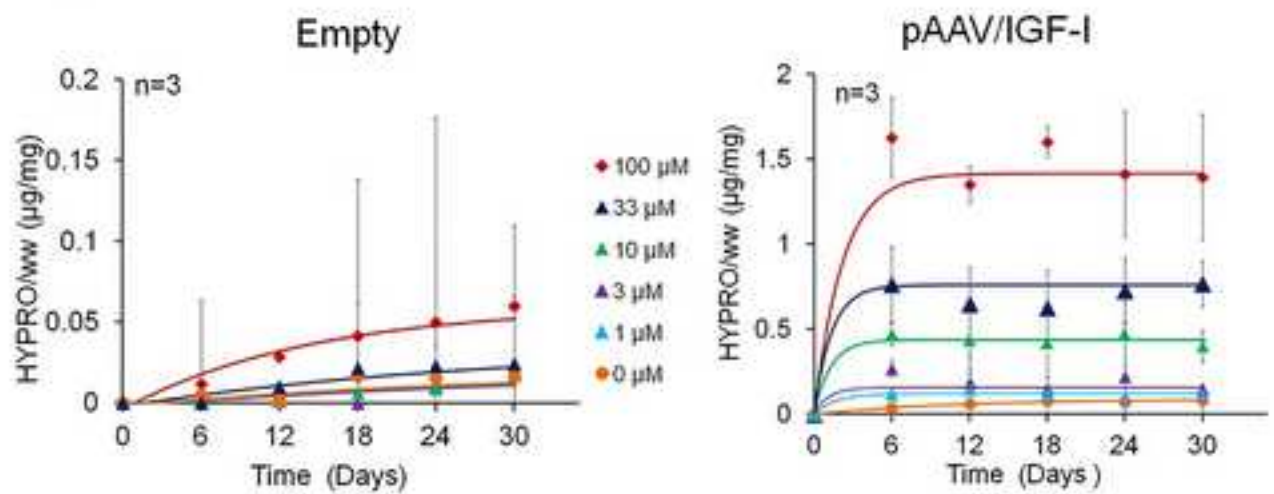


Matrix Synthesis

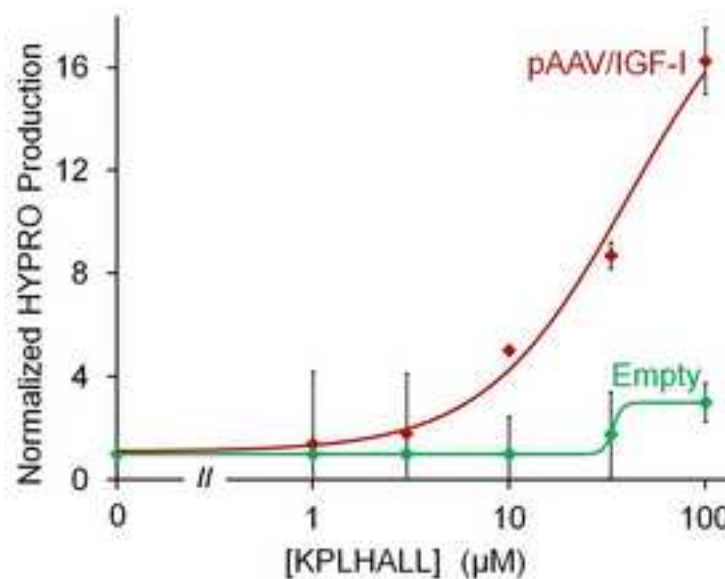
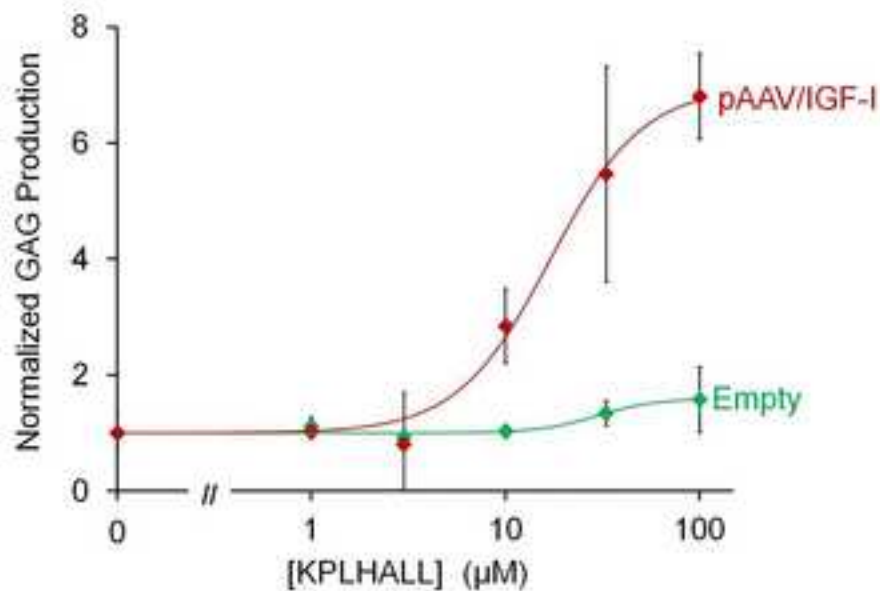
A) GAG



B) HYPRO

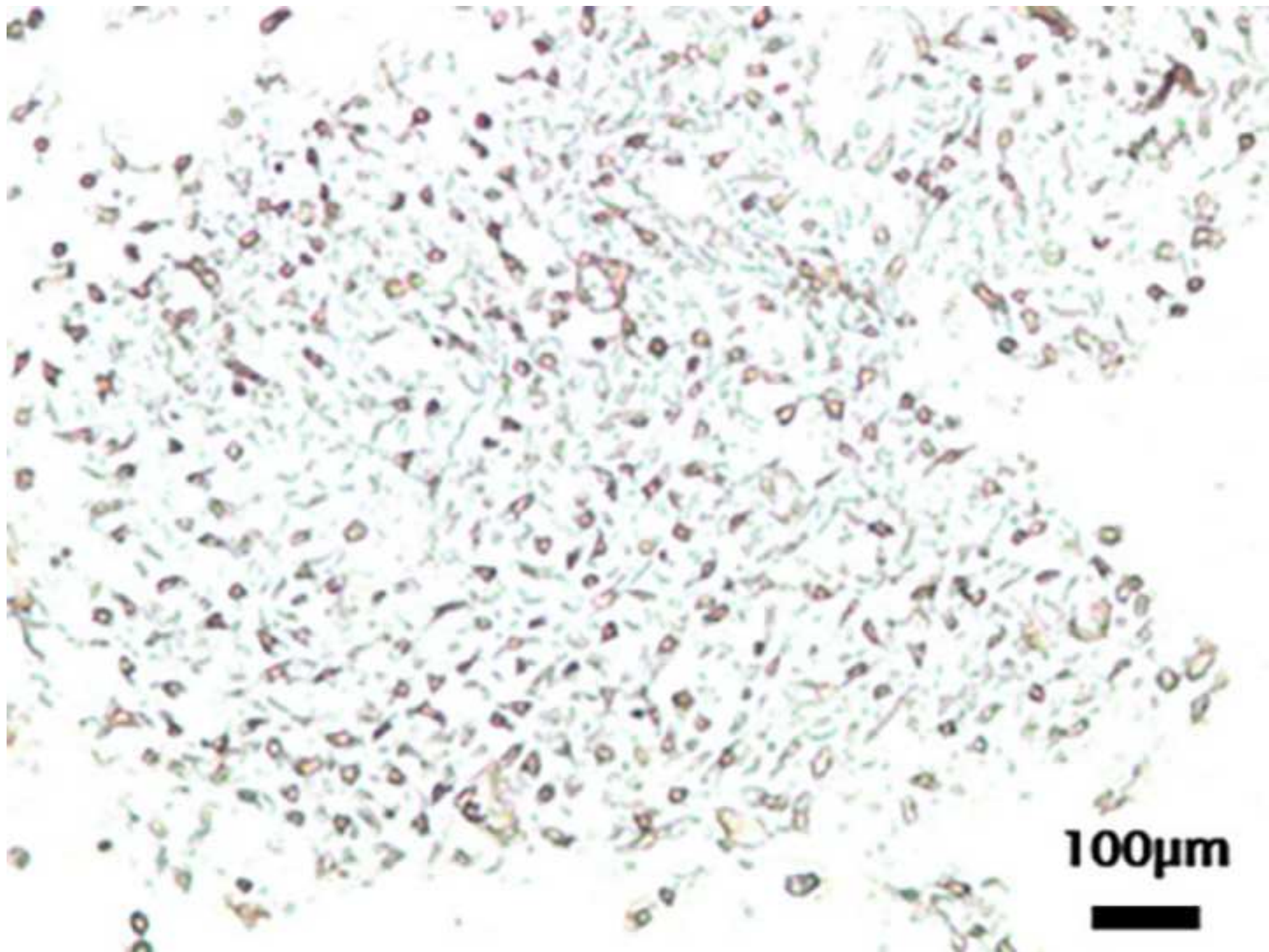


A) Dose Response



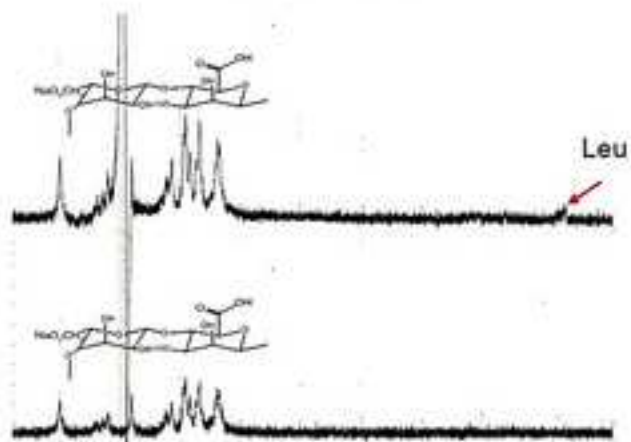
B) Dose Response Parameters

	GAG		HYPRO	
	pAAV/IGF-I	Empty	pAAV/IGF-I	Empty
EC ₅₀ (µM)	16.9±3.3	29.7± 9.2	41.0 ± 29.4	33.8±0.03
Max/Min	6.9±0.5 ^{~+}	1.6±0.1	19.4± 6.7 ^{%^}	3.0 ± 0.1
R ²	0.99	0.93	0.99	0.99

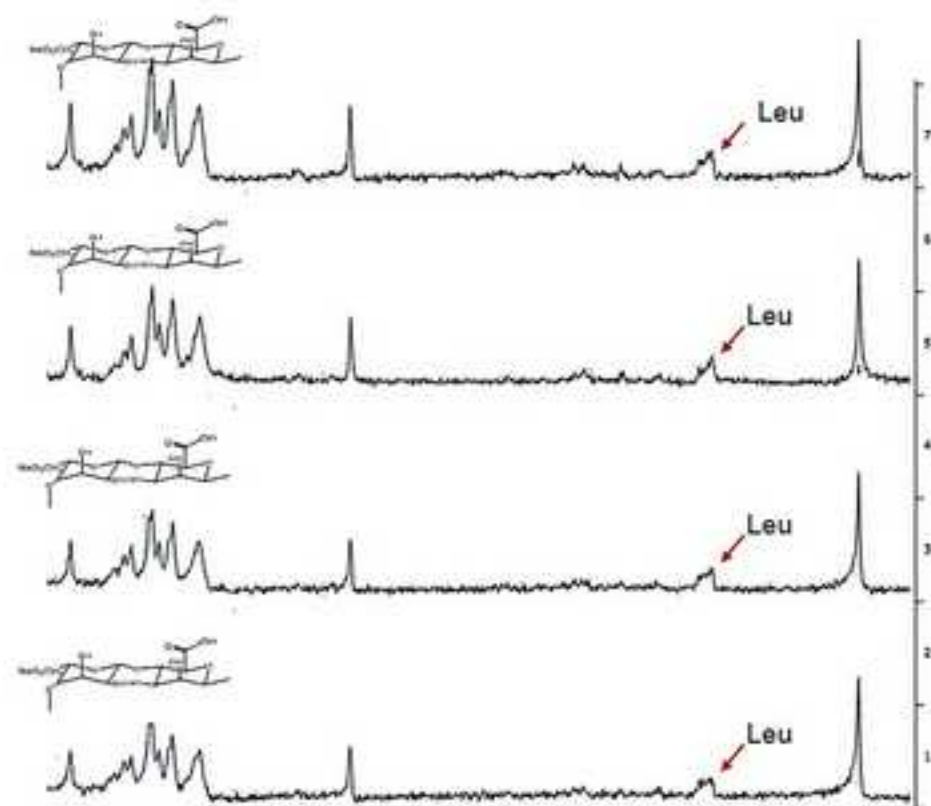


Diffusion Ordered Spectroscopy (DOSY)

Mixture



KPLHALL Alginate



Concentration of KPLHALL

0 μ M

1 μ M

3 μ M

10 μ M

33 μ M

100 μ M

Col II IHC
pAAV/IGF-I



